Fluorescence lifetime imaging of molecular rotors to map microviscosity in cells

(Invited Paper)

James A. Levitt[1], Marina K. Kuimova[2], Gokhan Yahioglu[2,3], Pei-Hua Chung[1], Klaus Suhling[1*], and David Phillips[2]

[1]*Department of Physics, King's College London, Strand, London WC2R 2LS, UK*

[2]*Department of Chemistry, Imperial College London, Exhibition Road, London SW7 2AZ, UK*

[3]*PhotoBiotics Ltd., 21 Wilson Street, London EC2M 2TD, UK*

[*]*E-mail: klaus.suhling@kcl.ac.uk*

Received June 13, 2010

Fluorescence liftime imaging (FLIM) of modified hydrophobic bodipy dyes that act as fluorescent molecular rotors shows that the fluorescence lifetime of these probes is a function of the microviscosity of their environment. Incubating cells with these dyes, we find a punctate and continuous distribution of the dye in cells. The viscosity value obtained in what appears to be endocytotic vesicles in living cells is around 100 times higher than that of water and of cellular cytoplasm.Time-resolved fluorescence anisotropy measurements also yield rotational correlation times consistent with large microviscosity values. In this way, we successfully develop a practical and versatile approach to map the microviscosity in cells based on imaging fluorescent molecular rotors.

OCIS code: 180.0180, 300.0300, 170.0170, 110.0110.

doi: 10.3788/COL20100810.0926.

Fluorescence imaging techniques are powerful tools in biological and biomedical sciences, because they are minimally invasive and can be applied to living cells and tissues. Fluorescence lifetime imaging (FLIM) in particular has emerged as a key technique to image the environment and interaction of specific proteins and dyes in living cells. It can report on photophysical events that are difficult or impossible to observe by fluorescence intensity imaging, because FLIM allows the separation of fluorophore concentration and quenching effects[1]. The vast majority of FLIM applications to date have been in the biomedical and life sciences, as the technique is non-destructive, minimally invasive and can be applied to living cells and tissues[2]. The most frequent use of FLIM is to detect Förster resonance energy transfer (FRET) to identify protein interactions or conformational changes of proteins[3,4]. Besides, applications in diverse areas such as forensic science[5], combustion research[6], luminescence mapping in diamond[7], microfluidic systems[8,9], art conservation[10], and lipid order problems in physical chemistry[11] have also been reported. Moreover, efforts are underway to use FLIM, possibly combined with endoscopy, for clinical diagnostics[12]. The power of FLIM lies in the ability to remotely monitor the local environment of a molecular probe independent of the fluorescence intensity or local probe concentration[1,13].

The fluorescence lifetime, $\tau_{\rm f}$, is the average time a fluorophore remains in the excited state after excitation, and is defined as the inverse of the sum of the rate parameters for all depopulation processes from the excited state[14,15]:

$$\tau_{\rm f} = \frac{1}{k_{\rm r} + k_{\rm nr}}, \tag{1}$$

where $k_{\rm r}$ is the radiative rate constant, and the non-radiative rate constant $k_{\rm nr}$ is the sum of the rate constant for internal conversion ($k_{\rm ic}$) and the rate constant for intersystem crossing to the triplet state ($k_{\rm isc}$): $k_{\rm nr} = k_{\rm ic} + k_{\rm isc}$. The fluorescence lifetime is related to the fluorescence quantum yield according to

$$\Phi_{\rm f} = \frac{k_{\rm r}}{k_{\rm r} + k_{\rm nr}} = k_{\rm r}\tau_{\rm f} \tag{2}$$

with $0< \Phi_{\rm f} <1$.

Diffusion is often an important rate-determining step in chemical reactions or biological processes, and viscosity is one of the key parameters affecting diffusion of molecules and proteins. In biological specimens, changes in viscosity have been linked to disease and malfunction at the cellular level, and signaling pathways along with protein-protein interactions are dependent on the transport of biomolecules in cells. Elucidation of intracellular reaction kinetics and mechanisms can thus potentially assist in development and understanding of the mechanisms of targeted therapies for cancer[16].

While methods to measure the bulk viscosity are well developed, macroscopic sample quantities are required, and mechanical or fluid dynamics approaches are used[17]. However, imaging the microviscosity, for example in single cells, remains a challenge. Indeed, viscosity maps of single cells have until recently been hard to obtain[18,19].

Rotational diffusion can be measured by time-resolved fluorescence anisotropy $r(t)$, which is defined as[14,15]

$$r\left(t\right) = \frac{I_{||}\left(t\right) - GI_{\perp}\left(t\right)}{I_{||}\left(t\right) + 2GI_{\perp}\left(t\right)}, \tag{3}$$

where $I_{||}(t)$ and $I_{\perp}(t)$ are the fluorescence intensity decays parallel and perpendicular to the polarization of the exciting light, and G accounts for different transmission and detection efficiencies of the imaging system at parallel and perpendicular polarization, and if necessary, an

appropriate background has to be subtracted[20]. For a spherical molecule, $r(t)$ decays as a single exponential and is related to the rotational correlation time θ according to

$$r(t) = (r_0 - r_\infty) \exp\left(-\frac{t}{\theta}\right) + r_\infty, \quad (4)$$

where r_0 is the initial anisotropy and r_∞ is the limiting anisotropy which accounts for a restricted rotational mobility. For a spherical molecule in an isotropic medium, θ is directly proportional to the viscosity η of the solvent and the volume V of the rotating molecule:

$$\theta = \frac{\eta V}{kT}, \quad (5)$$

where k is the Boltzmann constant and T is the absolute temperature. Thus imaging θ with time-resolved fluorescence anisotropy imaging (TR-FAIM) can measure the rotational mobility and diffusion of a fluorophore in its environment[20−24], as reviewed recently[25].

Molecular rotors are distinctive fluorescent molecules whose fluorescence lifetime is a function of the viscosity of their microenvironment[26−28]. Their radiative de-excitation competes with intramolecular twisting, which leads to non-radiative deactivation of the excited state. The rate constant for the latter pathway decreases in viscous media, such that the fluorescence lifetime τ_f and quantum yield Φ_f are high in viscous microenvironments and low in non-viscous microenvironments. Thus, the fluorescence lifetime can directly be converted into viscosity[29−31] using a calibration based on the Förster Hoffmann model[32]. This model states that the fluorescence lifetime, τ_f, of molecular rotors is a function of the viscosity, η, of their environment and can be described well by

$$\tau_\mathrm{f} = z k_\mathrm{r}^{-1} \eta^\alpha, \quad (6)$$

where z and α are constants[33].

Molecular rotors have been used to measure the microviscosity in polymers[34], sol-gels[31,35], micelles[36], ionic liquids[37−39], blood plasma[40], liposomes, and biological structures such as tubulin[41]. However, the main problem with fluorescence intensity-based measurements is distinguishing between viscosity and other factors which affect the fluorescence intensity, in particular the concentration of the fluorophore. A ratiometric approach, using probes that incorporate two linked independent fluorophores, one of which is unaffected by viscosity changes has been suggested to address this problem[42]. In this way, a calibration of the viscosity in fluorescence intensity measurements is possible and has been demonstrated. However, intensity-based measurements are prone to ambiguity in their analysis. If the rotors are distributed in a heterogeneous environment and exhibit multi-exponential decays, different viscosity and population distributions can result in the same fluorescence intensity.

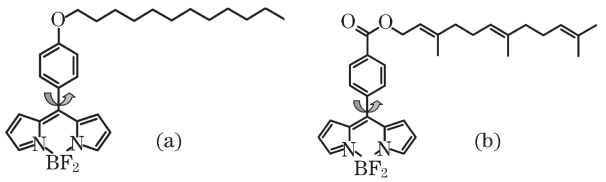

Fig. 1. Meso-substituted 4, 4′-difluro-4-bora-3a, 4adiaza-s-indacene molecular rotors. Long, hydrophobic tails are designed to render them membrance-soluble. (a) Alkyl chain; (b) farnesyl chain.

Alternatively, one can exploit the fluorescence lifetime of molecular rotors, which varies as a function of viscosity, according to Eq. (6). This approach does not require conjugation of the molecular rotor to another fluorescence label, decouples the influence of the viscosity on the fluorescence intensity from that of the rotor concentration, and also allows detection of heterogeneous rotor environments via multi-exponential fluorescence decays. In combination with FLIM, molecular rotors can be used to map microviscosity, particularly in a biological environment.

We recently synthesised meso-substituted 4, 4′-difluoro-4-bora-3a, 4adiaza-s-indacene rotors with long alkyl and farnesyl chains (see Fig. 1). They act as molecular rotors, and they can be used in combination with FLIM to map the microviscosity in living cells[29,30] and sol-gels[31]. The long, hydrophobic tails were designed to render the probes membrane-soluble and, hence, report on membranes and other hydrophobic domains in living cells. These dyes are extremely well suited for use as probes of biological environments (e.g., cells) because their optimum excitation and emission wavelengths are in the visible region, thus reducing the possibility of photodamage and phototoxicity.

FLIM experiments were performed by coupling a pulsed diode laser (Hamamatsu PLP-10) with the wavelength of 470 nm, pulse duration of $\sim$ 90 ps, and repetition rate of 20 MHz into an inverted laser scanning confocal microscope (Leica TCS SP2). Time-resolved fluorescence was measured through a bandpass filter (525±25 nm) using a photomultiplier and a time-correlated single-photon counting (TCSPC) card (SPC-830, Becker & Hickl). Line scan speeds for microscopy were 400 Hz and FLIM images were typically recorded in 300 s. Fluorescence measurements of the molecular rotors made in methanol/glycerol mixtures of different viscosities confirm that the fluorescence quantum yield increases dramatically with increasing solvent viscosity, as shown in Fig. 2(a). The fluorescence lifetime also increases with viscosity, from 0.7 ns in 20 cP to 3.8 ns in 950 cP for the molecular rotor with an alkyl chain (Fig. 1(a)). The observed increase in fluorescence intensity is consistent with the hindering of intramolecular rotation due to the high solvent viscosity, reducing the de-excitation via non-radiative pathways. The data obtained from the solvent mixtures are used to create a calibration graph according to the logarithmic version of Eq. (6):

$$\log \tau_\mathrm{f} = \alpha \log \eta + \log\left(\frac{z}{k_\mathrm{r}}\right), \quad (7)$$

allowing the conversion of fluorescence lifetime into viscosity, as shown in Fig. 2. A plot of log τ_f versus log η can be fitted well by a straight line with a slope of 0.5±0.1 for the molecular rotor with an alkyl chain and 0.75±0.1 for the molecular rotor with a farnesyl chain, in agreement with the literature data for molecular rotors in viscous media[32].

We incubated the molecular rotors in SK-OV-3 cells

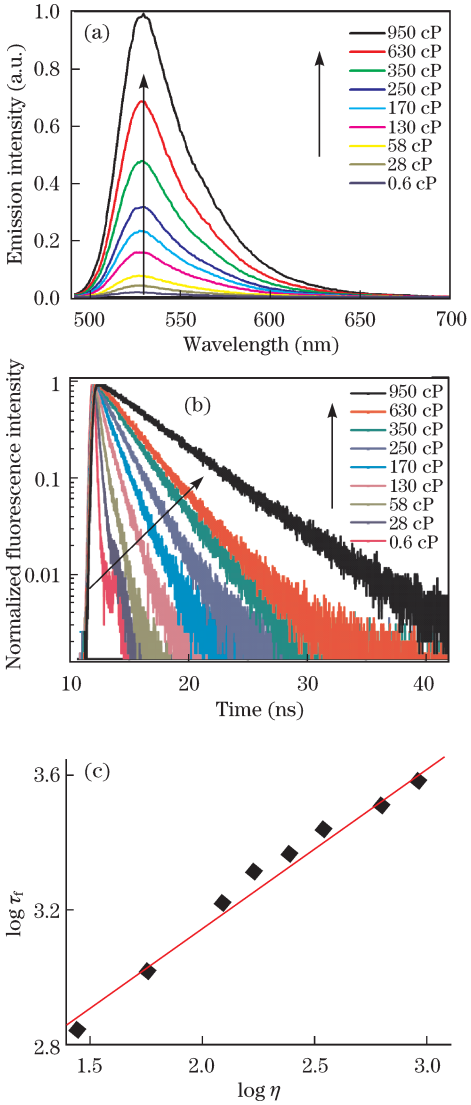

Fig. 2. (a) Fluorescence intensity and (b) fluorescence lifetime of the bodipy-based molecular rotor with an alkyl chain as a function of viscosity of the medium; (c) calibration graph for bodipy-based molecular rotors showing the logarithm of the fluorescence lifetime versus the logarithm of the viscosity of the medium. This graph allows the conversion of fluorescence lifetime into viscosity according to Eq. (6). (Colorful online)

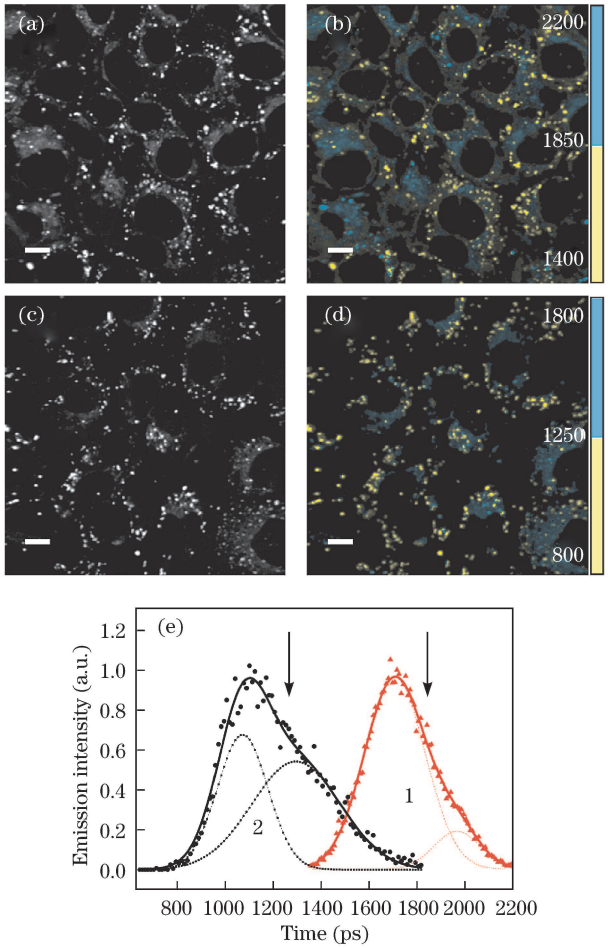

Fig. 3. Bodipy-based molecular rotors in cells. (a), (c) Fluorescence intensity and (b), (d) FLIM images for living SK-OV-3 human ovarian carcinoma cells are incubated with the rotors with (a), (b) the alkyl chain and (c), (d) the farnesyl chain. The fluorescence intensity images show a punctate and continuous distribution of the rotors. The fluorescence lifetime images show a short lifetime for the punctate distribution (1.4−1.85 ns) and a longer lifetime for the continuous distribution (1.85−2.2 ns). The FLIM images show the differences in fluorescence lifetime for the two dyes, recorded in the different regions of a cell. (The discrete color scale shows shorter lifetimes in yellow and longer lifetimes in blue online). The scale bars are 10 μm. (e) Fluorescence lifetime distribution histograms from FLIM measurements for the rotors with (1) the alkyl chain and (2) the farnesyl chain in intracellular environments. The asymmetric distributions can be adequately described and fitted by two contributions corresponding to a bimodal distribution of the fluorescence lifetimes. The arrows correspond to the cutoff in the discrete color scale bars for both molecular rotors with "short" and "long" fluorescence lifetimes arising from the punctate and cytoplasmic regions, respectively. Adapted from Ref. [29].

and found that they were readily taken up. The intracellular distribution patterns for both dyes are shown in Figs. 3(a) and (c)[29]. In addition to the bright punctate distribution of the molecular rotors in cells, we also observed regions of lower fluorescence intensity in what appears to be the cell cytosol. Due to the hydrophobic nature of both molecular rotors and the presence of the long tails, which render them membrane-soluble, we expect both molecular rotors to target the membrane domains of intracellular organelles.

FLIM images of SK-OV-3 human ovarian carcinoma cells incubated with both dyes are shown in Figs. 3(b) and (d)[29]. For both molecular rotors, the fluorescence decays in the image can be adequately fitted using a single exponential decay model. A histogram of the fluorescence lifetimes in the image is shown in Fig. 3(e). The histograms are asymmetric for both dyes, although pixel fits are mono-exponential. This is consistent with a bimodal distribution of fluorescence lifetimes across the image. The individual contributions to the histogram (best fit using Gaussian distributions) are at 1.7 and 2.0 ns for the molecular rotor with an alkyl chain and at 1.0 and 1.3 ns for the molecular rotor with a farnesyl chain. FLIM images with discrete color scales for the short and long lifetimes for each dye are shown in Figs. 3(b) and (d).

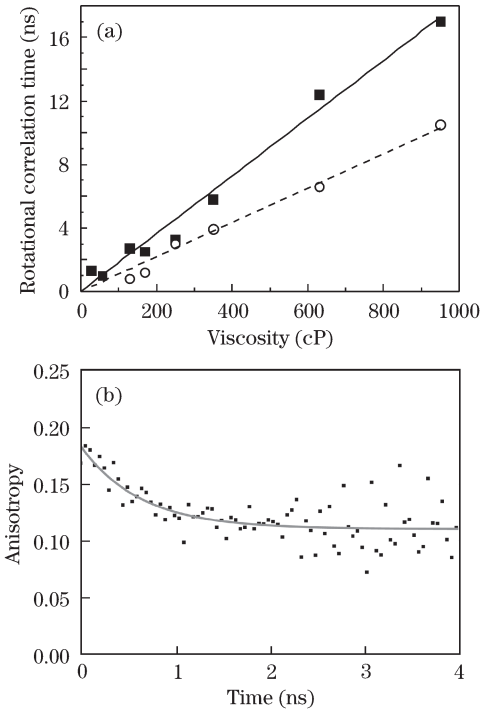

Fig. 4. (a) Plots of rotational correlation time versus viscosity for the molecular rotors with the alkyl chain (squares) and the farnesyl chain (circles) in methanol/glycerol solutions. The plots show linear fits to the data for both rotors, confirming the linear dependence of θ on η. Values of θ at a given η are found by fitting time-resolved anisotropy decays using Eq. (4). (b) Representative intracellular time-resolved fluorescence anisotropy decay from SK-OV-3 cells. A fit according to Eq. (4) yields a rotational correlation time of 590 ± 110 ps, which corresponds to a microviscosity of 60 cP. Adapted from Ref. [29].

From these images, it is clear that the measured short and long fluorescence lifetimes are organelle specific; that is, the short lifetimes are predominantly situated in the brighter puncta, and the longer lifetimes are found within what appears to be the cytosol. All the values for the fluorescence lifetimes detected for both molecular rotors from cells lie within the calibrated range of viscosities and, importantly, are within the regime of the good linear fit to the data for the calibration measurements, Fig. 2(c). According to the calibration curves for both molecular rotors, the shorter fluorescence lifetimes correspond to a viscosity 160 cP, whereas the longer fluorescence lifetimes correspond to the viscosity value of 260 cP. The dashed lines in Fig. 3 serve as indicators for the eye to demonstrate where the intracellular fluorescence lifetime contributions lie on the calibration curves and also demonstrate that the values obtained using both dyes do correspond to the same viscosity values.

To ensure that this high viscosity value does not result from the binding of the rotor to the intracellular targets, which could restrict the rotation of the phenyl group, we also performed time-resolved fluorescence anisotropy measurements of the molecular rotors in cells. These data measure the rotation of the entire molecule, and not simply the intramolecular motion. If binding occurs then an r_∞ may be observed which is a limiting anisotropy. This would not be detectable using steady-state anisotropy measurements, nor by lifetime meaurements alone. The rotational diffusion rate can be determined by polarization-resolved TCSPC. Time-resolved fluorescence anisotropy decays were recorded with viscosity varying from 28 to 950 cP for both rotors. The rotational correlation time θ of the molecular rotor with an alkyl chain increases linearly with solvent viscosity. Plots of rotational correlation time versus viscosity for both molecular rotors in methanol/glycerol solutions are shown in Fig. 4(a). The values were extracted from fits of the fluorescence anisotropy decays using Eq. (4) with a zero value for r_∞. The calibration graph for rotational correlation time versus viscosity can be used to calculate the effective microviscosity in cells.

A representative time-resolved fluorescence anisotropy decay for the molecular rotor with a farnesyl chain in SK-OV-3 cells is shown in Fig. 4(b). Regions of interest in the stained areas of the SK-OV-3 cells were scanned, and fluorescence lifetime measurements were recorded simultaneously for fluorescence polarized parallel and perpendicular to the polarization vector of the excitation beam. This was achieved using two photomultipliers with a polarizing beam splitter. The output from each detector was fed into the TCSPC card via a four-channel router (Becker & Hickl). From these data, the fluorescence anisotropy decay was extracted and fitted with a single exponential decay model according to Eq. (4). The measured rotational correlation time was 590±110 ps, which corresponds to a viscosity of 60 cP. This value, along with the value found from the fluorescence lifetime data, is significantly higher than that expected of the aqueous cytoplasmic region[18,43,44] but slightly lower than those found using fluorescence lifetime measurements. The differences between the values obtained by anisotropy and lifetime measurements may be due to deviation from the simple hydrodynamic model assumed for the anisotropy analysis in the cellular environment.

In conclusion, FLIM offers some key advantages over intensity-based measurements of molecular rotors, because it allows the separation of viscosity and probe concentration effects. The bodipy dyes can report the microviscosity via variations in their fluorescence lifetimes, and thus mapping the viscosity in cells can be carried out by FLIM. The bodipy's fluorescence properties and high cellular uptake make them ideal candidates for studies in biological systems. Our measurements using fluorescent molecular rotors confirm the heterogeneity in the viscosity in the stained regions. This result highlights the importance of spatially resolved microscopic scale measurements in biological environments. By tailoring the chemistry and delivery method of the molecular rotors, it may be possible to create microviscosity maps on the wide range of intracellular environments and targets on the basis of fluorescence lifetimes measured by FLIM, or ratiometric spectral imaging. In short, we have developed a practical and versatile approach to measuring the microviscosity of the environment of molecular rotors in cells.

M. K. Kuimova thanks the UK's Engineering and Physical Sciences Research Council (EPSRC) Life Sciences Interface Program for a personal Fellowship. We would

also like to acknowledge funding by the UK's Biotechnology and Biological Sciences Research Council (BBSRC). P.-H. Chung would like to acknowledge a King's College London Graduate School Studentship.

References

1. F. Festy, S. M. Ameer-Beg, T. Ng, and K. Suhling, Molecular Biosystems **3,** 381 (2007).
2. F. S. Wouters, Contemporary Physics **47,** 239 (2006).
3. E. A. Jares-Erijman and T. M. Jovin, Nature Biotechnol. **21,** 1387 (2003).
4. H. Wallrabe and A. Periasamy, Current Opinion in Biotechnol. **16,** 19 (2005).
5. D. K. Bird, K. M. Agg, N. W. Barnett, and T. A. Smith, J. Microsc.-Oxford **226,** 18 (2007).
6. T. Ni and L. A. Melton, Appl. Spectrosc. **50,** 1112 (1996).
7. G. Liaugaudas, A. T. Collins, K. Suhling, G. Davies, and R. Heintzmann, J. Phys. Condensed Matter **21,** 364210 (2009).
8. R. K. P. Benninger, O. Hofmann, J. McGinty, J. Requejo-Isidro, I. Munro, M. A. A. Neil, A. J. deMello, and P. M. W. French, Opt. Express **13,** 6275 (2005).
9. A. D. Elder, S. M. Matthews, J. Swartling, K. Yunus, J. H. Frank, C. M. Brennan, A. C. Fisher, and C. F. Kaminski, Opt. Express **14,** 5456 (2006).
10. D. Comelli, G. Valentini, R. Cubeddu, and L. Toniolo, Appl. Spectrosc. **59,** 1174 (2005).
11. D. M. Togashi, R. I. S. Romao, A. M. G. da Silva, A. J. F. N. Sobral, and S. M. B. Costa, Phys. Chem. Chem. Phys. **7,** 3875 (2005).
12. J. Requejo-Isidro, J. McGinty, I. Munro, D. S. Elson, N. P. Galletly, M. J. Lever, M. A. A. Neil, G. W. H. Stamp, P. M. W. French, and P. A. Kellett, Opt. Lett. **29,** 2249 (2004).
13. K. Suhling, P. M. W. French, and D. Phillips, Photochem. Photobiol. Sci. **4,** 13 (2005).
14. J. R. Lakowicz, *Principles of Fluorescence Spectroscopy* (3rd edn.) (Springer, New York, 2006).
15. B. Valeur, *Molecular Fluorescence* (Wiley, Weinheim, 2002).
16. M. K. Kuimova, S. W. Botchway, A. W. Parker, M. Balaz, H. A. Collins, H. L. Anderson, K. Suhling, and P. R. Ogilby, Nature Chem. **1,** 69 (2009).
17. E. Kaliviotis and M. Yianneskis, Proc. Inst. Mech. Eng. Part H J. Eng. Med. **221,** 887 (2007).
18. K. Luby-Phelps, S. Mujumdar, R. Mujumdar, and L. A. Ernst, Biophys. J. **65,** 236 (1993).
19. J. A. Dix and A. S. Verkman, Biophys. J. **57,** 231 (1990).
20. K. Suhling, J. Siegel, P. M. P. Lanigan, S. Lévêque-Fort, S. E. D. Webb, D. Phillips, D. M. Davis, and P. M. W. French, Opt. Lett. **29,** 584 (2004).
21. J. Siegel, K. Suhling, S. Lévêque-Fort, S. E. D. Webb, D. M. Davis, D. Phillips, Y. Sabharwal, and P. M. W. French, Rev. Sci. Instrum. **74,** 182 (2003).
22. A. H. A. Clayton, Q. S. Hanley, D. J. Arndt-Jovin, V. Subramaniam, and T. M. Jovin, Biophys. J. **83,** 1631 (2002).
23. D. S. Lidke, P. Nagy, B. G. Barisas, R. Heintzmann, J. N. Post, K. A. Lidke, A. H. A. Clayton, D. J. Arndt-Jovin, and T. M. Jovin, Biochem. Soc. Trans. **31,** 1020 (2003).
24. A. N. Bader, E. G. Hofman, P. Henegouwen, and H. C. Gerritsen, Opt. Express **15,** 6934 (2007).
25. J. A. Levitt, D. R. Matthews, S. M. Ameer-Beg, and K. Suhling, Current Opinion in Biotechnol. **20,** 28 (2009).
26. M. A. Haidekker and E. A. Theodorakis, Org. Biomol. Chem. **5,** 1669 (2007).
27. A. C. Benniston, A. Harriman, V. L. Whittle, and M. Zelzer, Eur. J. Org. Chem. **2010,** 523 (2010).
28. B. D. Allen, A. C. Benniston, A. Harriman, S. A. Rostron, and C. F. Yu, Phys. Chem. Chem. Phys. **7,** 3035 (2005).
29. J. A. Levitt, M. K. Kuimova, G. Yahioglu, P.-H. Chung, K. Suhling, and D. Phillips, J. Phys. Chem. C **113,** 11634 (2009).
30. M. K. Kuimova, G. Yahioglu, J. A. Levitt, and K. Suhling, J. Am. Chem. Soc. **130,** 6672 (2008).
31. G. Hungerford, A. Allison, D. McLoskey, M. K. Kuimova, G. Yahioglu, and K. Suhling, J. Phys. Chem. B **113,** 12067 (2009).
32. T. Föster and G. Hoffmann, Zeitschrift für Physikalische Chemie Neue Folge (in German) **75,** 63 (1971).
33. B. Wilhelmi, Chem. Phys. **66,** 351 (1982).
34. R. O. Loutfy, Pure Appl. Chem. **58,** 1239 (1986).
35. A. Rei, G. Hungerford, and M. I. C. Ferreira, J. Phys. Chem. B **112,** 8832 (2008).
36. K. Y. Law, Photochem. Photobiol. **33,** 799 (1981).
37. K. I. Gutkowski, M. L. Japas, and P. F. Aramendia, Chem. Phys. Lett. **426,** 329 (2006).
38. A. Paul and A. Samanta, J. Phys. Chem. B **112,** 16626 (2008).
39. J. Lu, C. L. Liotta, and C. A. Eckert, J. Phys. Chem. A **107,** 3995 (2003).
40. M. A. Haidekker, A. G. Tsai, T. Brady, H. Y. Stevens, J. A. Frangos, E. Theodorakis, and M. Intaglietta, Am. J. Physiol.-Heart and Circulatory Physiology **282,** H1609 (2002).
41. C. E. Kung and J. K. Reed, Biochemistry **28,** 6678 (1989).
42. M. Haidekker, T. P. Brady, D. Lichlyter, and E. A. Theodorakis, J. Am. Chem. Soc. **128,** 398 (2006).
43. N. Periasamy, M. Armijo, and A. S. Verkman, Biochemistry **30,** 11836 (1991).
44. K. Fushimi and A. S. Verkman, J. Cell Biol. **112,** 719 (1991).